

# 退火及热轧对碳钢-不锈钢爆炸焊接 复合板性能的影响

廖东波<sup>1</sup>, 查五生<sup>1</sup>, 李 伟<sup>1,2</sup>

(1. 西华大学 材料科学与工程学院, 成都 610039; 2. 宜宾北方鑫安复合材料有限公司, 宜宾 644221)

**摘 要:** 通过 EDS 线扫描分析、SEM 检测以及力学性能测定, 研究了碳钢-不锈钢爆炸焊接复合板在焊态、退火态以及热轧态的力学性能和微区组织特征, 分析了复合板元素过渡区域的特点。结果表明, 退火热处理以及热轧处理均降低了复合板的抗拉强度和屈服强度, 恢复了复合板的塑性以及韧性。复合板在焊态、退火态以及热轧态时的过渡区域具有不同的显微组织形态。退火后其过渡区域的波状界面结构与焊态基本一致, 过渡区域宽度约为 5  $\mu\text{m}$  左右, 而热轧成薄板后的复合板, 其过渡区域的波状界面消失, 过渡区域宽度变宽, 约为 20  $\mu\text{m}$ 。

**关键词:** 爆炸焊接复合板; 热轧; 退火; 力学性能; 显微结构

**中图分类号:** TG456.6 **文献标识码:** A **文章编号:** 0253-360X(2013)01-0109-04



廖东波

## 0 序 言

爆炸焊接是使用炸药作为能源进行的金属间焊接和生产金属基复合材料的一种很有实用价值的高新技术<sup>[1,2]</sup>。它的最大特点是在一瞬间能将相同的、特别是不同的和任意的金属组合, 简单、迅速和强固地焊接在一起<sup>[1]</sup>。它的最大用途是制造大面积的各种组合、各种形状、各种规格和各种用途的双金属及多金属复合材料<sup>[2]</sup>。爆炸焊接复合板存在的一个问题是难以按照预定要求厚度进行生产, 使得爆炸焊接复合板不能以一定规格厚度商品进入市场, 所以通常解决这个问题的方法是对焊后的复合板进行轧制<sup>[1]</sup>以获得各种厚度的复合板。文中以某公司爆炸焊接生产复合板为背景, 讨论了碳钢和不锈钢的爆炸焊接复合板的焊接工艺, 并分别分析了退火及热轧工艺对这种爆炸焊接复合板力学性能和结合界面处的微区组织的影响。

## 1 试验方法

试验中覆板采用了美国标准的 304 不锈钢, 牌号相当于中国标准的 0Cr18Ni9 不锈钢, 每块覆板的尺寸为 3 000 mm  $\times$  1 500 mm  $\times$  15 mm。基板采用了

Q235A、Q235B、Q345(16Mn)、20 钢等各型碳钢, 因 Q345 钢抗拉强度与覆板抗拉强度较接近, 故文中以 Q345 钢为主要基板材料。每块基板长宽尺寸与覆板相同, 规格为 3 000 mm  $\times$  1 500 mm  $\times$  45 mm。表 1 为覆板(304 不锈钢)和基板(Q345 钢)材料的参数。

表 1 爆炸焊接覆板材料和基板材料的参数

Table 1 Technical parameters of cover plate and base plate used for explosive welding

材料	厚度 $\delta/\text{mm}$	抗拉强度 $R_m/\text{MPa}$	断后伸长率 $A(\%)$	国家标准 材料
304	15	530	40	0Cr18Ni9
Q345	45	470 ~ 630	21 ~ 27	—

一般爆炸焊接工艺流程为: 覆板和基板材料准备及预处理—炸药、药框、间隙物和保护层准备—在沙土基础上进行装配—引爆进行爆炸焊接—复合板表面及外观检查—破坏性检验及无损探伤—热处理及轧制—校平、剪切或切削加工。根据此工艺流程, 在确定好覆板和基板材料参数、焊接用炸药参数以及覆板与基板之间的装配参数后, 实施了多次爆炸焊接过程, 中间经过多次修改参数, 最后得到了质量稳定可靠的复合钢板, 制取的焊接试样之一如图 1 所示。从图 1 中可以看出, 碳钢与不锈钢复合界面处, 出现了正弦波特征, 其波长约为 1 ~ 1.5 mm, 波高约为 200 ~ 400  $\mu\text{m}$ , 呈大波状界面<sup>[1]</sup>。界面处

的微观形貌质量良好,未发现明显裂纹及焊合不好的现象。

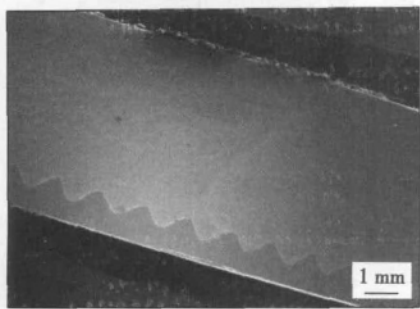


图 1 碳钢-不锈钢爆炸焊接界面 SEM 形貌  
Fig. 1 SEM photo of explosive welding interface

表 2 碳钢-不锈钢复合板的力学性能参数

Table 2 Mechanical properties of composite plate produced by explosive welding

状态	屈服强度 $R_{eL}$ /MPa	抗拉强度 $R_m$ /MPa	断后伸长率 $A$ (%)	内弯角 $\phi_1$ /( $^\circ$ )	外弯角 $\phi_2$ /( $^\circ$ )	冲击韧度 $a_{KV}$ /( $J \cdot cm^{-2}$ )
焊态	513	569	19.0	180	180	82
退火态	379	536	22.0	180	180	143
热轧态	353	457	34.4	180	180	157

由表 2 可见,焊态的复合板其抗拉强度比退火态和热轧态更高,主要因为爆炸焊接过程中发生了加工硬化,但复合板的冲击韧度和断后伸长率都较低。退火态的抗拉强度、屈服强度以及冲击韧度与热轧态的数据相比很接近,但热轧态断后伸长率最高。这说明退火热处理以及热轧处理均降低了复合板的抗拉强度和屈服强度,但恢复了复合板的塑性以及韧性。

## 2.2 碳钢-不锈钢复合板界面结合区的元素分布

试验中将焊态、退火态和热轧态的爆炸焊接复合板样品进行了界面处的 EDS 线扫描分析,如图 2,图 3 和图 4 所示,图 2、图 3 和图 4 中的扫描线表示的是某种元素相对强度,而非该元素的质量分数或原子分数,该图仍可用以说明各元素含量在结合界面处的变化趋势。

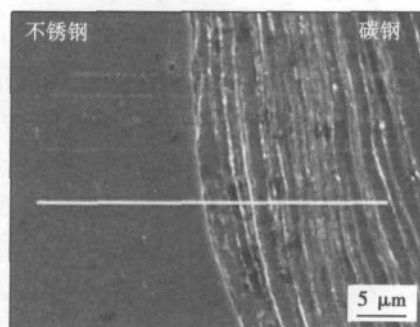
图 2 为焊态复合板界面处的 EDS 线扫描图谱,从不锈钢向碳钢扫描,在焊接界面处 Fe、Cr 和 Ni 元素含量均发生了较缓慢的变化,铁从碳钢侧向不锈钢侧扩散,而铬、镍从不锈钢向碳钢侧扩散,产生了厚度约为  $5 \mu m$  的过渡层。因此如前所述,这里所制得的爆炸焊接试样的特点是波状界面的波长约为  $1 \sim 1.5 mm$ ,波高约为  $200 \sim 400 \mu m$ ,过渡区域宽度约为  $5 \mu m$ ,与大波状界面<sup>[1]</sup>(波长为  $300 \mu m$ ,波高为  $100 \sim 150 \mu m$ ,过渡区域宽度为  $30 \mu m$ )基本一致,但最大的区别在于过渡区域宽度的不同。文中试验

试验中对爆炸焊接复合板分别进行了退火热处理及热轧处理。退火工艺为:将试件按制定好的升温速度升温至完全退火温度,保温时间为 3 h,随炉冷却。而热轧工艺为:首先将爆炸焊接复合板的坯板预热保温,然后将其热轧到  $4 \sim 10 mm$ ,热轧时的总压加率约为  $80\% \sim 90\%$ 。

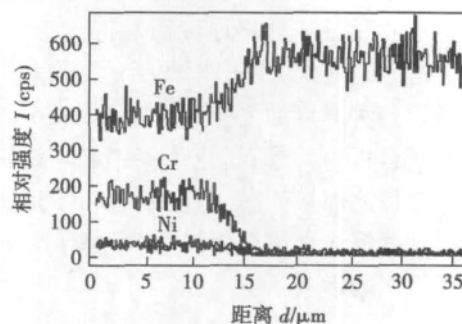
## 2 试验结果及分析

### 2.1 碳钢-不锈钢复合板的力学性能

在制备好焊态、退火态以及热轧态的复合板试样之后,分别检测了复合板在这 3 种状态下的抗拉强度、屈服强度和断后伸长率等力学性能,结果见表 2。



(a) 焊态线扫描位置示意图



(b) 焊态结合界面线扫描图谱

图 2 碳钢-不锈钢爆炸焊接结合界面 EDS 图谱

Fig. 2 EDS linear scanning photos of interface of explosive welded composite plate

条件下制得的试样其过渡区域宽度窄,比小波状界面<sup>[1]</sup>的过渡区域(宽度为  $15 \mu m$ )还要窄,而过渡区

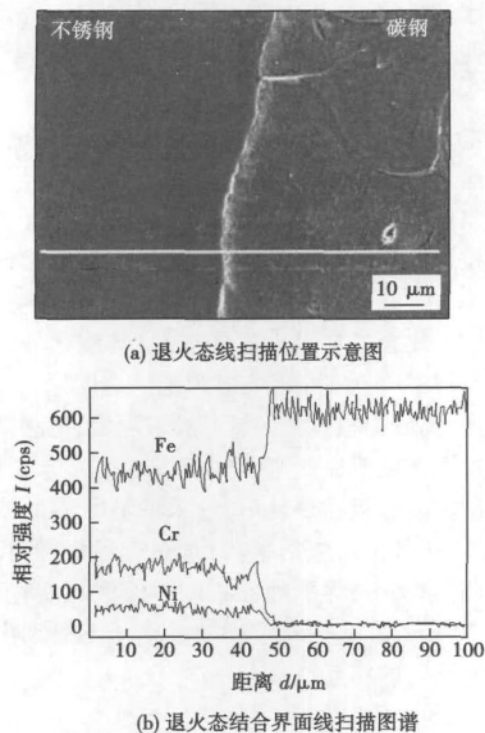


图 3 退火后碳钢-不锈钢爆炸焊接结合界面 EDS 线扫描图谱

Fig. 3 EDS linear scanning photos of interface of explosive welded composite plate after annealing

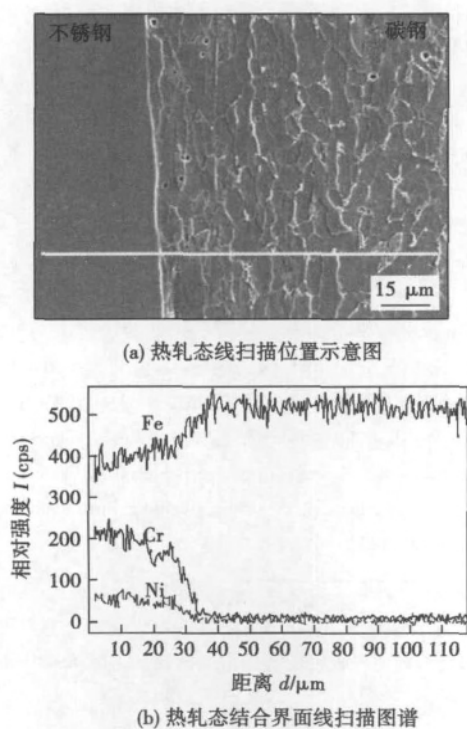


图 4 热轧后碳钢-不锈钢爆炸焊接结合界面 EDS 图谱

Fig. 4 EDS linear scanning photos of interface of explosive welded composite plate after rolling

域越窄,说明结合界面的熔化量小,焊接质量好<sup>[13-5]</sup>。

图 3 为退火态复合板界面处的 EDS 线扫描图谱。分析图谱发现,过渡区域的宽度仍然约为 5  $\mu\text{m}$  与焊态(退火前)相比较,过渡区域宽度并没有因为退火热处理而扩大,这主要是因为固态下原子扩散系数相对较小,扩散量有限。

图 4 为热轧态复合板界面处的 EDS 线扫描图谱。界面处 Fe、Cr 和 Ni 元素出现了更宽的过渡区,过渡区域尺寸大大增加,变为 20  $\mu\text{m}$  左右。因热轧的加工率大,热轧后板材总厚度由焊接前的 60 mm 变薄到 4~10 mm,但过渡区域宽度不是变小而是变大,这表明碳钢与不锈钢在热轧过程中再次出现了界面元素的相互扩散。

### 2.3 碳钢-不锈钢复合板过渡区的显微组织

图 5 为焊态、退火态和热轧态的碳钢与不锈钢复合板结合界面处的 SEM 扫描的微观组织形貌。图 5 中的亮色线条为碳钢晶粒的晶界,即腐蚀侧为碳钢,未腐蚀侧为不锈钢。

图 5a 为焊态复合钢板界面处的微观组织形貌,图 5a 中碳钢侧晶粒呈扁平状,出现了纤维组织,离界面的距离越近,晶粒越扁平。这充分说明在爆炸焊接过程中界面附近的金属层发生了剧烈的塑性伸长变形,且越靠近界面,伸长程度越大。爆炸焊接开始之前,碳钢与不锈钢的表面呈平行状。爆炸焊接过程中随着炸药的爆炸产生强烈的爆炸波,覆板随爆炸波向基板冲击和挤压,从而实现相互焊合。复合板的横截面上,界面由直线变成正弦波纹,界面的长度显著增加。在界面附近的金属层中,界面长度的增加量随距离界面的远近发生变化,界面的表层增加量最大,而较远部位增加量较少。爆炸焊接后界面长度的增加由界面两侧的基板和覆板发生塑性伸长变形来补偿,在微观结构上表现为界面附近的晶粒被拉长成为扁平状,离界面的距离越近晶粒越扁平。为承受拉伸的塑性变形,爆炸焊接复合材料必须具有良好的塑性,碳钢与不锈钢都具有这种性能,能够作为覆板和基板使用。

图 5b 为退火态复合钢板界面处的微观组织形貌。从图 5b 中看出,热处理后复合钢板正弦波纹的界面仍然存在,清晰可见,但纤维组织消失,出现了等轴晶粒,且距离界面较近的区域晶粒较粗大,中心部位晶粒尺寸相对较小。说明爆炸焊接复合板在经过再结晶温度退火热处理后,碳钢和不锈钢均发生了再结晶现象,在爆炸焊接中由于晶粒变形产生的纤维状结构基本消失,变形基体中扁平的晶粒重新生成无畸变的新的等轴晶粒,且晶粒大小均匀。

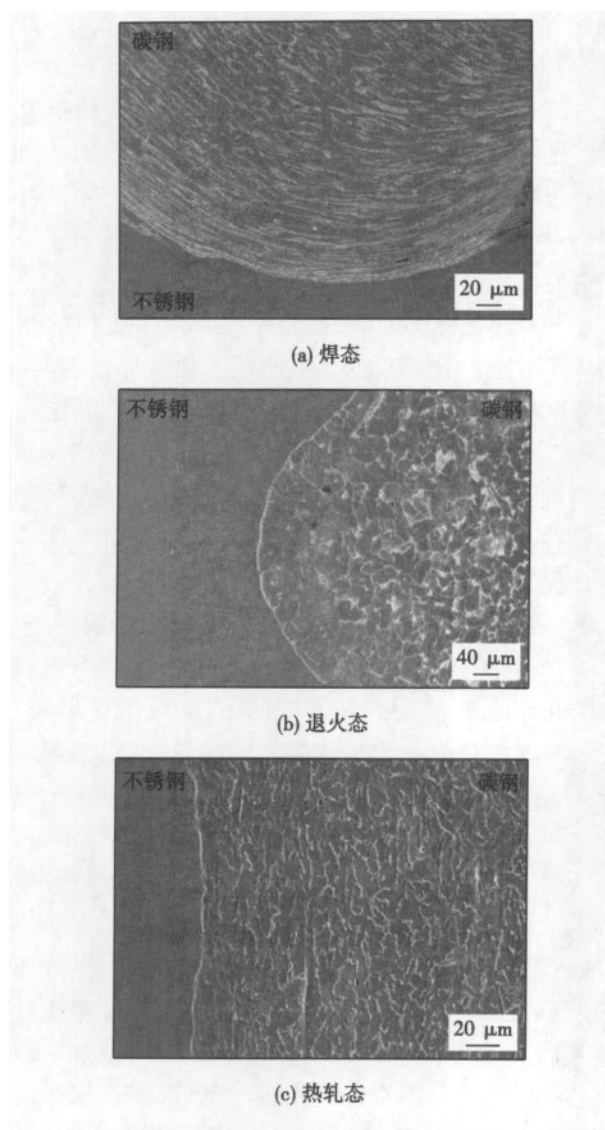


图 5 碳钢 - 不锈钢爆炸焊接界面 SEM 形貌

Fig. 5 Micrographs of interface of explosive welded composite plate

界面处的再结晶晶粒的尺寸大于试样其它部位晶粒的尺寸,是因为界面处存在着更高的形核能,在再结晶过程中促使了晶粒的长大。

图 5c 为热轧态复合钢板界面处的微观组织形貌。从图 5c 中可以看出,由于热轧时的加工率很大,所以热轧后复合钢板波状界面基本消失,原来的波状界面几乎完全变成平直状界面,且碳钢与不锈钢之间的界面同焊态和退火态相比略显模糊。热轧过程中虽伴随有动态再结晶,但晶粒仍被拉长成扁平状,且越靠近界面,晶粒的伸长量越大,晶粒越扁平。由于碳钢 - 不锈钢复合板是在高温下热轧,热轧过程中伴随有动态再结晶,塑性变形过程中发生的加工硬化被再结晶消除,复合板被软化,所以与焊

态相比,热轧态具有较低的抗拉强度和显著提高的断后伸长率。

### 3 结 论

(1) 退火热处理以及热轧处理均降低了复合板的抗拉强度和屈服强度,恢复了复合板的塑性以及韧性。

(2) 复合板在退火热处理后,其波状界面几乎保持与焊态一致,其纤维组织消失,出现了等轴晶粒,且距离界面较近的区域晶粒较粗大,退火热处理未使过渡区域明显变宽,仍为 5  $\mu\text{m}$ 。

(3) 复合板在热轧后,原来的波状界面变为平直,晶粒仍被拉长成扁平状,越靠近界面,伸长量越大,晶粒越扁平,界面处元素的过渡区域变宽,增加到约 20  $\mu\text{m}$ ,表明热轧过程中碳钢与不锈钢出现了界面元素间的相互扩散。

### 参考文献:

- [1] 王耀华. 金属板材爆炸焊接研究与实践[M]. 北京: 国防工业出版社, 2007.
- [2] 中国机械工程学会焊接学会. 焊接手册(第1卷, 焊接方法及设备)[M]. 北京: 机械工业出版社, 2001.
- [3] 史长根, 王耀华, 蔡立良, 等. 爆炸焊接界面的结合机理[J]. 焊接学报, 2002, 23(2): 55 - 58.  
Shi Changgen, Wang Yaohua, Cai Ligen, *et al.* Bonding mechanism of interface in explosive welding[J]. Transactions of the China Welding Institution, 2002, 23(2): 55 - 58.
- [4] 陈晓强, 张可玉, 詹发民, 等. 线状爆炸焊接结合界面的显微分析[J]. 焊接学报, 2008, 29(9): 105 - 108.  
Chen Xiaoqiang, Zhang Keyu, Zhan Famin. Micro analysis of bonding interfaces with seam explosive welding[J]. Transactions of the China Welding Institution, 2008, 29(9): 105 - 108.
- [5] 廖东波, 查五生, 李 伟. 碳钢 - 不锈钢爆炸焊接复合板界面的显微结构[J]. 焊接学报, 2012, 33(5): 99 - 102.  
Liao Dongbo, Zha Wusheng, Li Wei. Microstructure of stainless steel-carbon steel composite plates produced by explosive welding[J]. Transactions of the China Welding Institution, 2012, 33(5): 99 - 102.

作者简介: 廖东波,男,1978 年出生,硕士,讲师。主要从事焊接工艺及设备方面的科研和教学工作。发表论文 3 篇。Email: ddlliao\_20@163.com

通讯作者: 查五生,男,教授。Email: zhaowusheng684@hotmail.com

Zhiping ( Tianjin Key Laboratory for Civil Aircraft Airworthiness and Maintenance , Civil Aviation University of China , Tianjin 300300 , China) . pp 93 – 96

**Abstract:** Two kinds of WC-10Co-4Cr coatings with different particle-density were deposited on 300M steel by high-velocity oxygen fuel ( HVOF ) technology. The microstructure and properties of WC-10Co-4Cr coatings were assessed by scanning electron microscope ( SEM ) , X-ray diffraction ( XRD ) and micro-hardness tester. The corrosion resistance of the two kinds of coatings in a 3.5% NaCl solution was investigated by polarization test and immersion test. The results indicated that the porosity ratio of high particle-density coating was 1.52% , which was 1.95 times as big as that of low particle-density coating. In the NaCl solution , the value of passivation current density of high particle-density coating was  $3.2 \mu\text{A}/\text{cm}^2$  , which was 2.67 times as big as that of low particle-density coating. Therefore , low particle-density coating exhibited superior corrosion resistance than high particle-density coating due to its less porosity.

**Key words:** particle-density; high-velocity oxygen fuel; WC-10Co-4Cr coating; porosity ratio; corrosion resistance

#### Improved ICP registration in 3-D model reconstruction

TU Zhiqiang<sup>1</sup> , ZHANG Ke<sup>1</sup> , YANG Chenglong<sup>2</sup> , ZHU Xiaopeng<sup>1</sup> , HUANG Jie<sup>1</sup> ( 1. Shanghai Key Laboratory of Laser Manufacturing & Material Modification , Shanghai Jiaotong University , Shanghai 200240 , China; 2. Dalian Shipbuilding Industry Group Co. , Ltd. , Dalian 116005 , China) . pp 97 – 100

**Abstract:** One algorithm to automatically register point cloud data in 3-D model reconstruction was proposed. In the algorithm , the initial registration transformations were firstly calculated according to the curvature and normal vector of the point cloud. Then the best initial registration transformation was selected by geometric hashing method and the initial registration was completed by this transformation. Next , the ICP ( iterative closest point ) algorithm was improved by redefining the nearest point: For one measured point of *A* , the nearest three points in *B* point cloud were firstly found; the triangle was formed by this three points and the foot point of this triangle was taken as nearest point of measured point. Then the improved ICP algorithm was used for accurate secondary registration. Finally , this algorithm was used to register the point data in previous model. And the results show this algorithm has the better performance in registration accuracy.

**Key words:** point cloud registration; iterative closest point; 3D reconstruction; laser remanufacturing

#### Analysis on microstructure and mechanism of extrusion-resistance welding for Cu-Al casing pipe

ZHAO Yue<sup>1</sup> , ZUO Tiejun<sup>2</sup> , LING Yong<sup>3</sup> , ZUO Ke<sup>1</sup> , WANG Xin<sup>1</sup> ( 1. School of Materials Science and Engineering , Ocean University of China , Qingdao 266100 , China; 2. Qingdao Haiqing Machinery Plant , Qingdao 266021 , China; 3. Belgian National Industry Research Institute , Zwijnaarde 9359052 , Belgium) . pp 101 – 104

**Abstract:** The extrusion-resistance welding was developed to join Cu-Al casing pipe. The welded joints have characteristics of high cleanliness and high peel strength , without assistants and filling material. This technology has been widely used in refrigeration industry for the welding of various sized pipes. The microstructure of the Cu-Al joint was analyzed by SEM and TEM. The results show that Cu-Al joints made by extrusion-resistance weld-

ing are mainly composed of solid solution and intermetallic compounds ( IMCs ) (  $\alpha$  ,  $\text{Al}_2\text{Cu}$  and  $\text{Al}_4\text{Cu}_9$  ) . The high temperature generated by the resistance heat and pressure leads to the formation of new phase. The pressure exerted by the mandril extrudes the brittle composition , and enlarges the contact area , which makes the columnar grain easily formed.

**Key words:** Cu-Al pipe; extrusion-resistance welding; refrigerant pipeline; microstructure

#### Influence of laser offset on microstructure and mechanical properties of Ti/Al dissimilar joint by laser welding

SONG Zhihua<sup>1</sup> , WU Aiping<sup>1</sup> , YAO Wei<sup>2</sup> , ZOU Guisheng<sup>1</sup> , REN Jialie<sup>1</sup> , WANG Yongyang<sup>2</sup> ( 1. Key Laboratory for Advanced Materials Processing Technology of the Ministry of Education , Tsinghua University , Beijing 100084 , China; 2. Beijing Hangxing Technology Development Co. , Ltd. , Beijing 100013 , China) . pp 105 – 108

**Abstract:** Laser welding of TA15 and 5A06 alloys with 3 mm in thickness was conducted by focusing laser beam on titanium side , and the aluminum was melted through the heat conduction from titanium side. The effect of laser offset distance on microstructure and mechanical properties of the dissimilar butt joint was investigated. When the laser offset is 0.1-0.4 mm , fusion welded joint is formed. When the laser offset is 0.5 mm , fusion welded joint is formed on the upper side of the joint accompanying with Ti-Al intermetallic compounds. Welded-brazed joint is formed on the middle and bottom side of the joint accompanying with continuous Ti-Al intermetallic compounds layer with 1  $\mu\text{m}$  thickness. The tensile strength of joints firstly increased and then decreased with the laser offset increasing. The highest average tensile strength of the joint reaches 181 MPa when the laser offset distance is 0.5 mm. The joints partly fracture in Ti-Al intermetallic compounds at the interface , and partly fracture at the fusion zone of aluminum alloy.

**Key words:** titanium alloy; aluminum alloy; laser welding; microstructure; mechanical property

#### Effects of annealing and hot-rolling on properties and microstructure of explosion-welded composite steel plate

LIAO Dongbo<sup>1</sup> , ZHA Wusheng<sup>1</sup> , LI Wei<sup>1 2</sup> ( 1. College of Materials Science and Engineering , Xihua University , Chengdu 610039 , China; 2. Yibin North Xin'an Composite Materials Co. , Ltd. , Yibin 644221 , China) . pp 109 – 112

**Abstract:** The mechanical properties and microstructure of as-welded , as-annealed and as-rolled stainless steel-carbon steel composite plates produced by explosive welding were investigated by SEM and mechanical tests. The element diffusion of transition layer formed in explosive welding was measured by EDS linear scanning. The results show that both the annealing and the hot-rolling can reduce the tensile strength and yield strength of the composite plates , but improve the ductility and toughness of the composite plates. The microstructure of the transition layer of as-welded , as-annealed and as-rolled composite plates are different. The wavy interface of the as-annealed composite plate is similar to that of as-welded composite plates. The diffusion layer with thickness of only about 5  $\mu\text{m}$  is formed. For as-rolled composite plate , the wavy interface disappears and the diffusion layer enlarges to about 20  $\mu\text{m}$  in width.

**Key words:** explosion-welded composite plate; hot rolling; annealing; mechanical properties; microstructure